Journal of Applied Electrochemistry (2007) 37:331–337
DOI 10.1007/s10800-006-9261-5

Electrochemical oxidation of *p*-sulfonated calix[8]arene

MING CHEN, HUI-LAN WANG, JING GU and GUO-WANG DIAO*
College of Chemistry & Chemistry Engineering, Yangzhou University, Yangzhou, Jiangsu, 225002, P.R. China
*(*author for correspondence, tel.: +865147975587, fax: +865147975244, e-mail: gwdiao@yzu.edu.cn)*

Received 25 October 2005; accepted in revised form 10 October 2006

Key words: Electrochemistry, Diffusion activation energy, Diffusion coefficient, *p*-sulfonated calix[8]arene

Abstract

The water-soluble *p*-sulfonated sodium salt of calix[8]arene (III) was synthesized. The product was characterized by FT-IR, NMR and UV–Vis spectra. Then the electrochemical behaviors of *p*-sulfonated sodium salt of calix[8]arene in NaAc + HAc (pH = 4) buffer solution was studied. In aqueous solution, *p*-sulfonated calix[8]arene can be oxidized when the potential is more than 0.7 V vs SCE. It was confirmed that the reaction was a two-electron irreversible electrochemical reaction. The transfer coefficient, α, was measured as 0.7. At 25°, the diffusion coefficient of *p*-sulfonated calix[8]arene was determined as 8.6×10^{-7} cm^2 s^{-1}. The diffusion activation energy of *p*-sulfonated calix[8]arene was 18.9 kJ mol^{-1} at pH = 4.

1. Introduction

Calix[*n*]arenes are cyclic oligomers synthesized by condensation of a *p*-alkylated phenol and formaldehyde. Although all members of the series from $n = 4$ to 20 are known, even oligomers (tetramers, hexamers, octamers, etc.) are easier to synthesize than odd ones. Recently, calixarenes have received much attention as a fascinating class of receptors with a hydrophobic cavity which has the ability to interact by hydrogen bonding, C–H···π and N^+–H···π with a great variety of guests, from apolar compounds such as fullerenes [1] to charged molecules such as metallic cations [2, 3], organic [4] and inorganic anions [5]. This versatility makes the calixarene family the third major class of macrocyclic binding agents after the crown-ethers and the cyclodextrins [6, 7].

Among the functionalized calixarenes, the water-soluble calixarenes are of particular interest because of their potential use as simulation enzyme models [8], as catalysts [9] and as mobile phase in chromatography [10] and capillary electrophoresis [11]. The electrochemical properties of calixarenes are of interest for two reasons. First, they can provide insights into the binding of both electroinactive and electroactive guest species, thus providing a route to the label-free electrochemical monitoring of calixarene-based recognition events. Second, they can open up new avenues for immobilization of these receptor molecules onto surfaces, for example, by electrosorption or electroderivatization, with potential applications in sensing and molecular separations. Pailleret et al. [12, 13] reported the electrochemical characteristics of *p*-sulfonated calix[6]arene. We made a study of the electrochemical properties of *p*-sulfonated calix[4]arene [14] and *p*-sulfonated calix[6]arene [15]. The results showed that both *p*-sulfonated calix[6]arene and *p*-sulfonated calix[4]arene could be oxidized at 0.7–0.8 V vs SCE. Both anodic waves came into existence due to the oxidation of the phenolic group. The results showed that it was easier to oxidise *p*-sulfonated calix[4]arene than *p*-sulfonated calix[6]arene. This paper deals with the electrochemical behavior of *p*-sulfonated calix[8]arene. *p*-Sulfonated calix[8]arene is similar to *p*-sulfonated calix[4]arene and *p*-sulfonated calix[6]arene, which can also be oxidized at a potential of 0.7–0.9 V vs SCE. Compared with both *p*-sulfonated calix[4]arene and *p*-sulfonated calix[6]arene, the oxidation of *p*-sulfonated calix[8]arene is more difficult. The kinetic parameters, such as n, the number of the electrons transferred in the electrochemical reaction, D_R, the diffusion coefficient of *p*-sulfonated calix[8]arene and the diffusion activation energy, E_d are reported.

2. Experimental

All reagents used were analytical grade. *p*-Sulfonated calix[8]arene was synthesized by the following route shown in Figure 1.

p-Tert-butyl-phenol reacted with paraformaldehyde in NaOH solution with xylene as solvent. According to Gutsche et al. [16–18], the product is *p*-tert-butyl calix[8]arene (I). According to Gutsche et al. [19, 20], II was obtained. III was synthesized by the reactions of calix[8]arene with concentrated H_2SO_4[21–23] (Figure 1). At the end of the reaction the mixture was neutralized by $BaCO_3$. The crude product was obtained when a clean

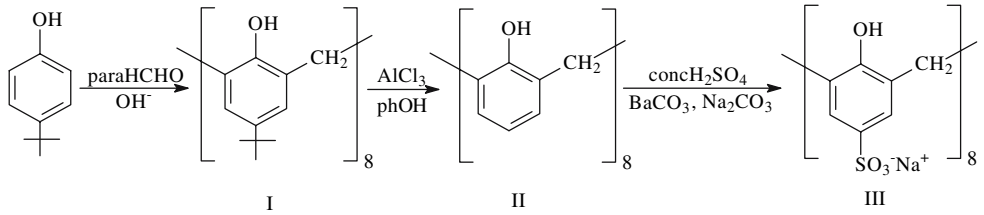

Fig. 1. The route for the synthesis of *p*-sulfonated calix[8]arene.

neutral solution was evaporated in a rotating evaporator. The crude product was dissolved in heated water. The pH of the solution was adjusted to 9 with Na_2CO_3 aqueous solution. A white precipitate, the final product III, was obtained by adding methanol to the above solution. The IR spectra of I, II, III were taken by FTIR spectrometer (Bruker TENSOR 27 FTIR spectrometer) with a KBr film and shown in Figure 2. The IR spectra of I and III were similar to those reported in the literature [18]. Figure 2a shows the FTIR spectrum of *p*-tert-butyl calix[8]arene; the band observed at 2957 cm^{-1} was assigned to *p*-tert-butyl stretching vibration. Comparing the spectrum shown in Figure 2a with that in Figure 2b, it was clear that the characteristic peaks of *p*-tert-butyl shown in curves (a) completely disappeared at curve (b) while other peaks remained unchanged, which meant that debutylation was successful and II was obtained. In Figure 2c, the bands appeared at 1180 and 1052 cm^{-1}, which was assigned to the characteristic peaks of SO_3^- and was consistent with the results of Shinkai [22]. Therefore, III was the object product that would be used in the next experiment.

^1H NMR spectra were recorded on a Bruker AV 600-MHz instrument. The values of chemical shifts of I were 9.65(8H, s, ArOH), 7.24(16H, s, ArH), 4.37(d, 8H, $CH_{2(a)}$), 3.50(d, 8H, $CH_{2(b)}$), 1.27(s, 72H, $C(CH_3)_3$). The results were in agreement with the literature [16]. The values of chemical shifts of III were 7.34(s, 16H, ArH) and 3.73(s, 16H, $ArCH_2Ar$), which was also similar to those reported in the literature [22]. From the NMR results, the peak of *p*-tert-butyl did not present itself in III, which further proved that III was the object product.

The UV–vis spectrum of III was taken using a UV-2550 (Shimazu, Japan) double-beam spectra photometer with a stoppered quartz cell with an optical path length of 1 cm. The wavelength of maximum absorption was 284 nm. At 25° and 284 nm, the molar absorbance coefficient of III was 1.2×10^5 L mol^{-1} cm^{-1}. The molar absorbance coefficient of *p*-sulfonated calix[4]arene [14] and *p*-sulfonated calix[6]arene were 6.0×10^3 L mol^{-1} cm^{-1} and 5.5×10^4 L mol^{-1} cm^{-1}, respectively. It was clear that the molar absorbance coefficient of III was larger than that of *p*-sulfonated calix[4]arene and *p*-sulfonated calix[6]arene, which indicated that the molar absorbance coefficient of *p*-sulfonated calixarene was enhanced with the numbers increasing of phenol units.

All electrochemical experiments were carried out with a CHI660a electrochemical workstation (Zhenghua, Shanghai) with a three-electrode cell. A Glassy carbon disc electrode (diameter: 3 mm) or micro-platinum disc electrode (diameter: 20 μm) were used as the working electrode. The reference electrode was a saturated calo-

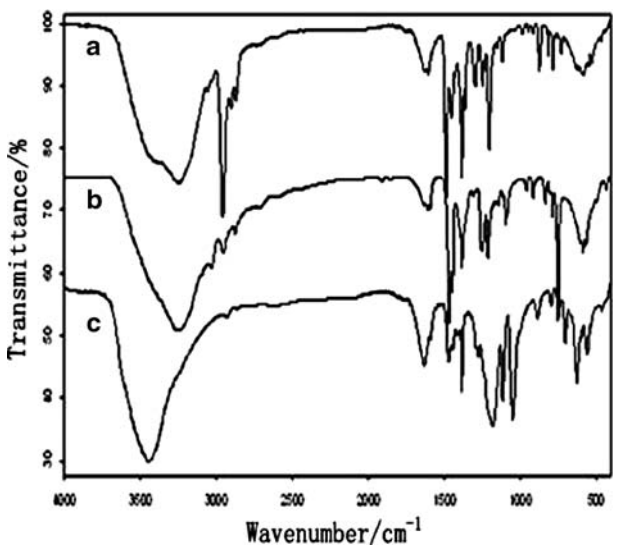

Fig. 2. IR spectra for *p*-tert-butyl calix[8]arene(I)(a), calix[8]arene(II)(b), *p*-sulfonated calix[8]arene (III)(c).

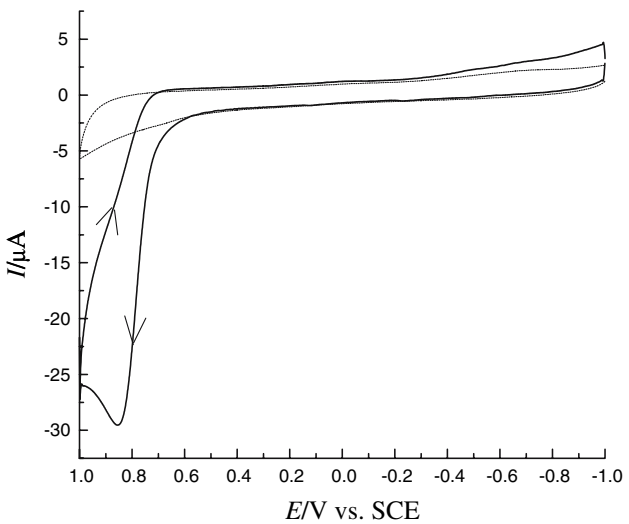

Fig. 3. Voltammograms of III; 25°, 0.1 V s^{-1}, 1×10^{-3} M III + 0.5 M HAc + 0.5 M NaAc (pH = 4); dashed line: background; solid line: solution containing III.

mel electrode (SCE). All potentials reported in this paper are against SCE. A platinum wire was used as the counter electrode. The aqueous electrolyte solutions were prepared by dissolving III in 0.5 M HAc + 0.5 M NaAc buffers in which the pH was measured as 4.0 using a PHs-25 pH-meter (Leizi Instrumental Factory, Shanghai). The working electrode was polished to a mirror finish with 0.05 μm alumina aqueous slurry and rinsed with water in an ultrasonic cleaning bath before.

3. Results and discussion

At first, the working electrode was cycled in 0.5 M HAc + 0.5 M NaAc buffers between −1.0 and 1.0 V (vs SCE) until a stable reproducible background voltammogram shown in Figure 3 as the dashed line was obtained. There is no electrochemical reaction in the plain buffer solution in our experimental potential window. After measurement of the background, the working electrode was immediately moved into an electrolyte solution containing III to study the electrochemical behavior. The voltammograms of III are also shown in Figure 3 (solid line). There is only one anodic wave when the potential is scanned from −1.0 to 1.0 V vs SCE. Compared with *p*-sulfonated calix[4, 6]arenes [14, 15], the anodic peak potential of III shifts in positively, which means that it is more difficult for the oxidation of III than *p*-sulfonated calix[4]arene and *p*-sulfonated calix[6]arene.

The voltammograms recorded for multi-cycles are shown in Figure 4. The anodic current decreased with increasing cycle number and tended to a stable value. This may be due to the poor solubility of the oxidized state of III which is similar to that for the electrochemical oxidation of *p*-sulfonated calix[4, 6]arenes reported previously [14, 15]. In fact, if the potential acting on the working electrode is cut off and the working electrode is kept in the electrolyte solution for several minutes, the electrode surface resumes its initial state. The reason for the current decrease with cycle number is probably due to diffusion layer depletion during the repeated scans. Therefore, in the following discussion, the current is taken in the first cycle.

3.1. *Measurements of n, D_R, and* α

As shown in Figure 5, both anodic peak potential, E_p and peak current, I_p are affected by scan rate, v. According to Nicholson [24], for an irreversible anodic reaction, the relationship between E_p and ln$v$ is linear and can be described as follows

$$E_p = E^{0'} + \frac{RT}{\alpha n_a F}\left[0.780 + \ln\left(\frac{D_R^{1/2}}{k^0}\right) + \ln\left(\frac{\alpha n_a F v}{RT}\right)^{1/2}\right] \quad (1)$$

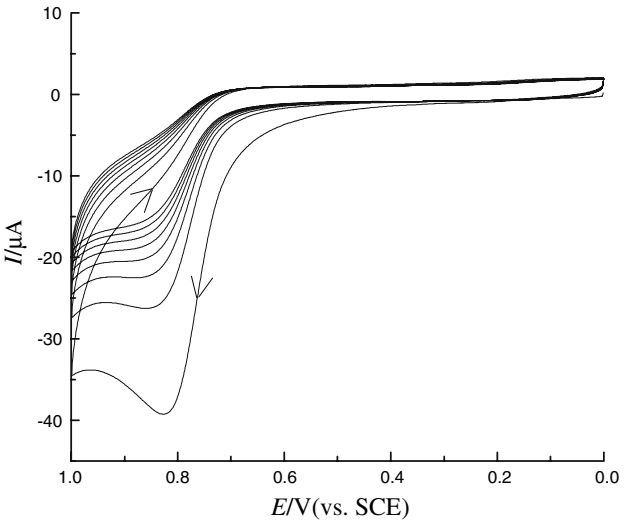

Fig. 4. Voltammogram of III for multi-cycles; 25°, 0.01 V s^{-1}, 1 × 10^{-3}M III + 0.5M HAc + 0. 5M NaAc; Voltammograms from bottom to top were obtained at first to eighth cycle.

where $E^{0'}$ is the formal standard potential, n_a the number of the electrons transferred in rate determining step and α the transfer coefficient. The plot of E_p vs ln$v$ is shown in Figure 6. A straight line is obtained which shows that the electrochemical reaction of III in the present conditions is irreversible. From the slope of the straight line the product of α and n_a was evaluated as 1.4.

On the other hand, I_p, the peak current for an irreversible electrochemical reaction can be described by the following formula

$$I_p = -(2.99 \times 10^5) n(\alpha n_a)^{1/2} A c_R^* D_R^{1/2} v^{1/2} \quad (2)$$

where n is the total number of electrons transferred in the electrochemical reaction and c_R^* is the initial concentration of III. According to Equation 2, at a given

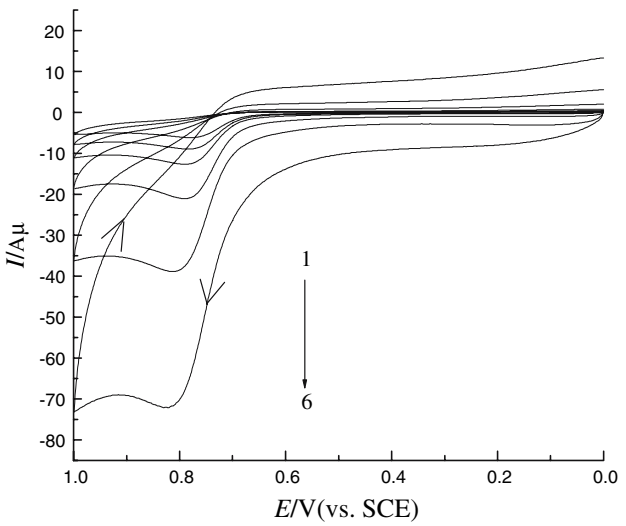

Fig. 5. Cyclic voltammograms of III at different scan rates; 25°, 1 × 10^{-3} M III + 0.5 M HAc + 0.5 M NaAc; v(V s^{-1}): (1) 0.005, (2) 0.01, (3) 0.02, (4) 0.05, (5) 0.2, (6) 0.5.

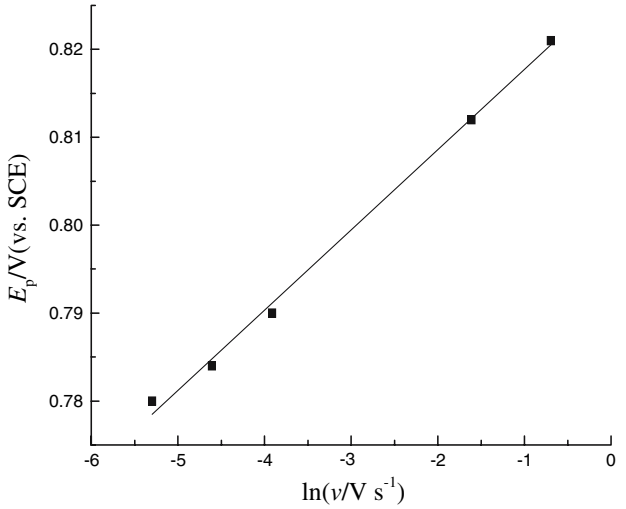

Fig. 6. Relationship between the peak potential and the natural logarithm of scan rate. The experimental conditions are the same as those described in Figure 4.

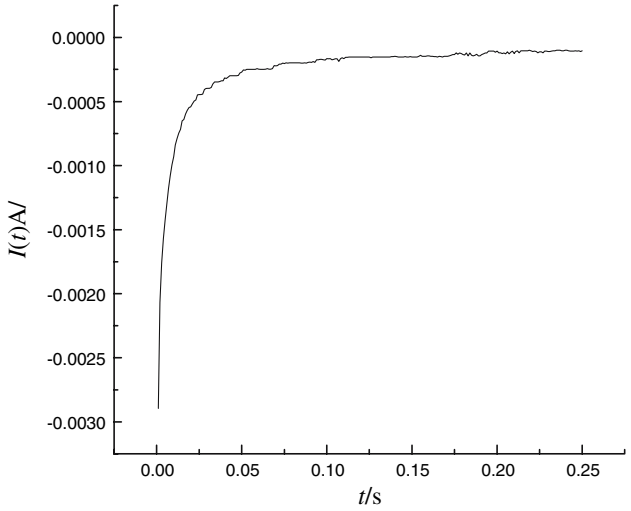

Fig. 8. Current, $I(t)$ of III vs time, t at 25°; 1×10^{-3}M III + 0.5M HAc + 0.5M NaAc, E stepped from 0 to 1.0 V.

initial concentration of III, the plot of I_p vs $v^{1/2}$ should be a straight line. Figure 7 shows the experimental results. From the slope of the straight line, the value of $[n(n_a\alpha)^{1/2}(D_R)^{1/2}]$ was evaluated as 1.9×10^{-3} cm s$^{-1/2}$. Combining it with the value of $n_a\alpha$, $nD_R^{1/2}$ was evaluated as 1.5×10^{-3} cm s$^{-1/2}$.

The value of $nD_R^{1/2}$ can also be measured by chronoamperometry. The current response is shown in Figure 8 when potential was stepped from 0 to 1.0 V (vs SEC). According to the Conttrell equation [24], the relationship between $I(t)$ and the inverse of the square root of time, $t^{-1/2}$ is linear and can be described as follows

$$I(t) = \frac{nFAD_R^{1/2}c_R^*}{\pi^{1/2}t^{1/2}} \tag{3}$$

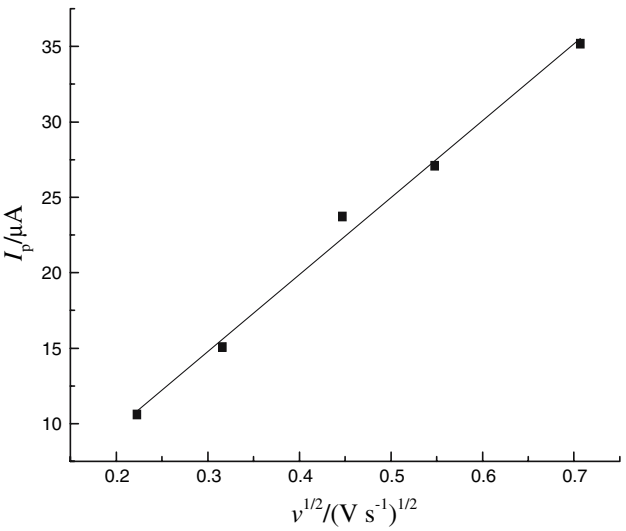

Fig. 7. Relationship between the peak current I_p and the square root of scan rate $v^{1/2}$. The experimental conditions are the same as those described in Figure 4.

The plot of $I_{(t)}$ vs $t^{-1/2}$ is shown in Figure 9 and a straight line is obtained. From the slope of the straight line, the product of $nD_R^{1/2}$ was evaluated as 1.3×10^{-3} cm s$^{-1/2}$, which coincided with that measured by plotting I_p vs $v^{1/2}$. The average value of $nD_R^{1/2}$ was taken as 1.4×10^{-3} cm s$^{-1/2}$.

To calculate the value of n and D_R, a steady state voltammogram was measured with an ultramicro platinum disc serving as working electrode (radius $r = 10$ μm). The experimental result is shown in Figure 10. The value of $nD_R$was evaluated as 1.3×10^{-6} cm^2 s^{-1} using $I_l = 4nFD_Rc_R^*r$ [24]. Combining the value of $nD_R^{1/2}$ described previously, D_R can be calculated as 8.6×10^{-7} cm^2 s^{-1}. The diffusion coefficients of *p*-sulfonated calix[4]arene [14] and *p*-sulfonated calix[6]arene [15] were 3.1×10^{-5} cm^2 s^{-1} and 1.4×10^{-6} cm^2 s^{-1}, respectively. It is clear that the diffusion coefficient of *p*-sulfonated calix[8]arene is the lowest of the three. Apparently, the diffusion coefficient of *p*-sulfonated calixarene

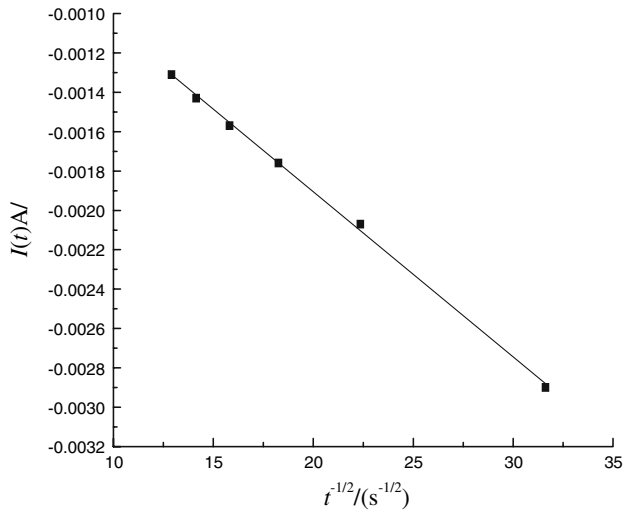

Fig. 9. Relationship between $I(t)$ and $t^{1/2}$.

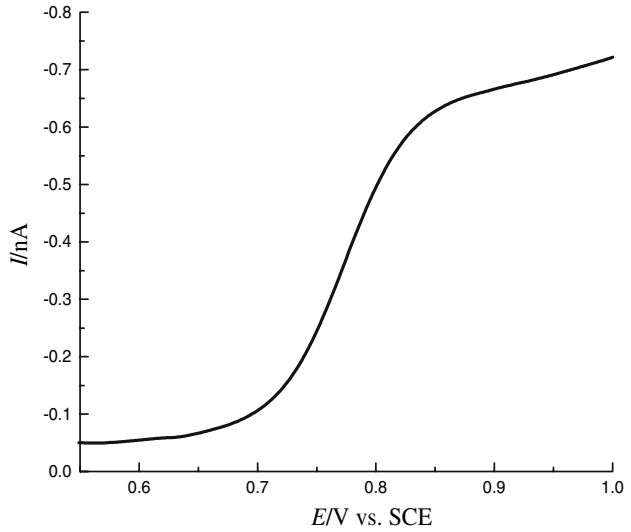

Fig. 10. Steady state voltammogram of III on ultramicro platinum disc electrode; $v = 10$ mV s^{-1}, the other experimental conditions are the same as those described in Figure 4.

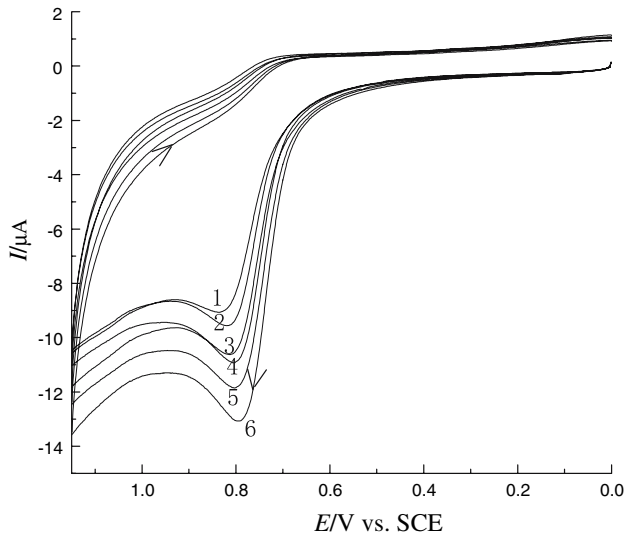

Fig. 11. Cyclic voltammograms of III at different temperatures; 5×10^{-4} M III + 0.5 M HAc + 0.5 M NaAc; temperatures (°): (1)20, (2)25, (3)30, (4)35, (5)40, (6)45.

decreased in the order *p*-sulfonated calix[4]arene, *p*-sulfonated calix[6]arene and *p*-sulfonated calix[8]arene, which may be due to the volume increase. The value of n was evaluated as 2. The positive charge was distributed on the whole calixarene molecule. Thus the oxidation of III in 0.5 M HAc + 0.5 M NaAc buffer solution is a two-electron transfer electrochemical reaction. Assuming $n = n_a$, the value of the transfer coefficient α is 0.7, which is quite similar to those of *p*-sulfonated calix[4, 6]arene.

3.2. *Temperature dependence*

Figure 11 shows the voltammograms of III at different temperatures. It is clear that both peak current, I_p, and peak potential, E_p, are affected by temperature. At high temperature the peak potential shifts in the negative direction. Meanwhile the current increases with temperature, which suggests that the oxidation of III is easier at high temperature. Taking account of n_a, α as independent of T, then according to Nicholson, the peak current, I_p at different temperatures should be described as follows

$$I_p = -0.4958nFA\left(\frac{\alpha n_a F}{RT}\right)^{1/2} c_R^* D_R^{1/2} v^{1/2} \quad (4)$$

From Equation (4), the diffusion coefficient, D, of III at different temperatures can be evaluated. The relationship between D and temperature can be expressed as follows

$$\log D = -\frac{E_d}{2.303RT} + \log D_\infty \quad (5)$$

where E_d is the activation energy of diffusion of III, D_∞ the diffusion coefficient of III at infinite temperature. Plotting log D vs the inverse of temperature, a straight line is obtained (see Figure 12). The value of E_d, was calculated as 18.9 kJ mol^{-1} at pH = 4.

3.3. *Effect of acidity*

The cyclic voltammograms of III at different acidities are shown in Figure 13, where Na_2SO_4 is the supporting electrolyte. The acidity of the solution was adjusted by H_2SO_4 or NaOH. At pH < 8, the anodic peak potential shifts negatively with the increases of pH, then becomes almost constant with further pH increase. Generally speaking, the peak potential is strongly affected by acidity at low pH. On the other hand, the peak current increases with increase in pH when pH < 8. The lower the pH, the more the number of protonated phenolic oxygen atoms in calixarene. The first ionization process of III can be described as follows

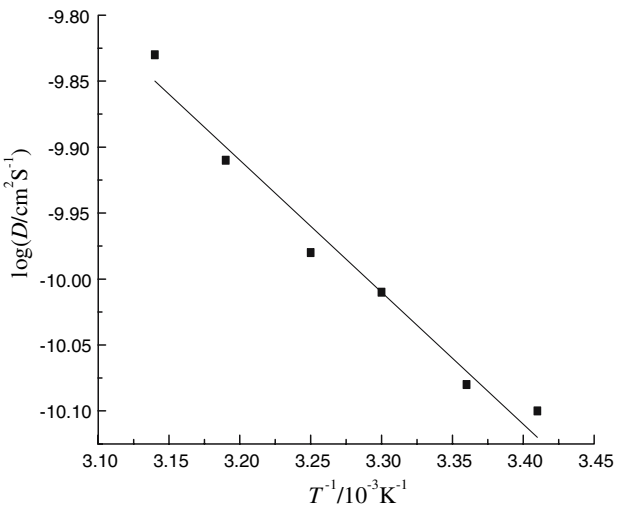

Fig. 12. Relationship between log D and $1/T$. $v = 100$ mV s^{-1}.

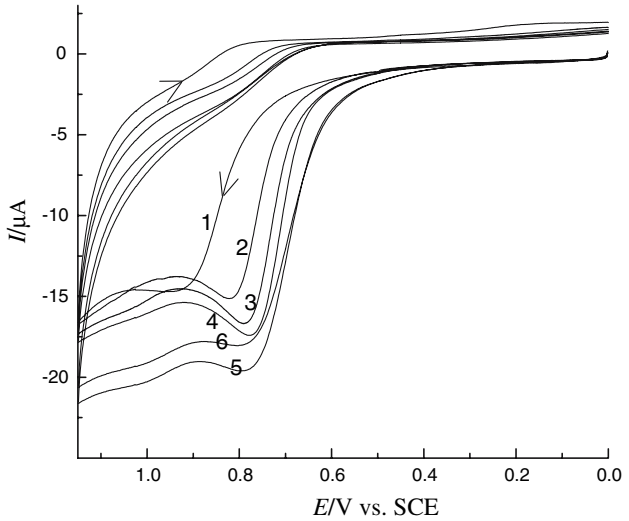

Fig. 13. Cyclic voltammograms of III at different acidities; 25° 0.01 V s^{-1}, 2×10^{-4} M III + 0.2 M Na_2SO_4; pH: (1) 2.5, (2) 4, (3) 5, (4) 6, (5) 8, (6) 10.

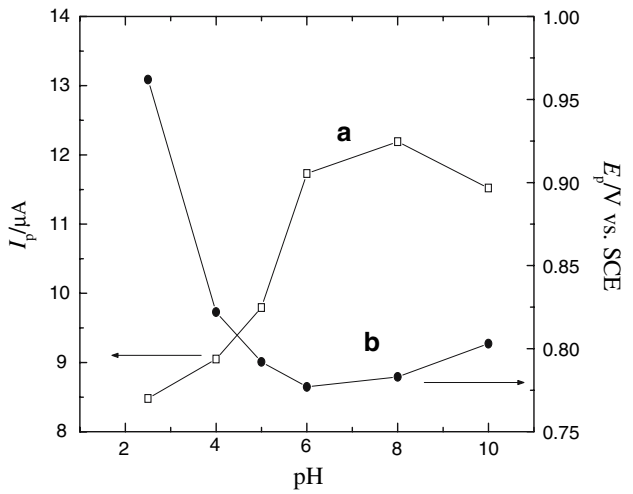

Fig. 14. Values of E_p and I_p at different pH. 25°, 2×10^{-4} M III + 0.2 M Na_2SO_4.

$$HA \rightleftharpoons H^+ + A^{-1} \quad (6)$$

where III is replaced by the symbol HA. The pK_a of III was determined as 8, which is smaller than that of phenol (pK_a = 9.95) [25]. Therefore, at low pH the anodic process observed in Figure 13 is due to the oxidation of the phenol units in III. But at high pH, the anodic wave is due to the oxidation of the phenolate anion. The anodic peak potential moves slightly negatively with increase in pH because phenolate is easier to oxidize than the corresponding phenol. When pH > 8, $[A^{-1}]$:[HA] > 1, most phenol units release their protons and become phenolate anions. Therefore, it can be assumed that there is no significant affect for E_p and I_p when pH > 8. However, as shown in Figure 14, both E_p and I_p are almost independent of pH when pH is higher than 6. Although the oxidization of *p*-sulfonated calixarene depends on pH, the exact mechanism is still unknown at present. Further work on the electrochemical oxidization of *p*-sulfonated calixarene is necessary.

4. Conclusions

In 0.5 M HAc + 0.5 M NaAc buffers, *p*-sulfonated calix[8]arene can be oxidized. The anodic peak potential is 0.83 V (vs SCE) at 25° at pH = 4.0. The anodic peak potential is affected by acidity and temperature. E_p is proportional to ln*v*, which shows that the oxidation of III is a totally irreversible process. The number of electrons transferred in the electrochemical reaction is 2. The transfer coefficient is 0.7. The diffusion coefficient of III is 8.6×10^{-7} cm^2 s^{-1}. The diffusion activation energy of III is 18.9 kJ mol^{-1} at pH = 4.

Acknowledgements

The authors acknowledge financial support from the National Natural Science Foundation of China (Grant No. 20373060), the Natural Science Foundation of the Educational Committee of Jiangsu Province of China (Grant No. 03KJB150151), and the Fund for an Academic Leader of QingLan Project of Institutions of Higher Learning in Jiangsu Province of China, which is a source for training upcoming scientists. The authors also acknowledge financial support from the Foundation of Jiangsu Provinicial Key Program of Physical Chemistry in Yangzhou University.

References

1. S. Kunsági-Máté, K. Szabó, I. Bitter, G. Nagy and L. Kollár, *Tetrahedron Lett*. **45** (2004) 1387.
2. Y. Liu, H. Wang, L.H. Wang and H.Y. Zhang, *Thermochim. Acta* **414** (2004) 65.
3. D.B. Isabelle, H. Hatem, O. Farhana and L. Roger, *C.R.Chimie*. **8** (2005) 881.
4. K. Lang, P. Cuřínová, M. Dudič, P. Prošková, I. Stibor, V. Šťastný and P. Lhoták, *Tetrahedron Lett*. **46** (2005) 4469.
5. A.K. Jain, V.K. Gupta, L.P. Singh, P. Srivastava and J.R. Raisoni, *Talanta* **65** (2005) 716.
6. A.F. Danil de Namor, R.M. Cleverley and M.L. Zapata-Ormachea, *Chem. Rev*. **98** (1998) 2495.
7. Y. Liu, C.C. You and H.Y. Zhang, *Supermolecular Chemistry* (NanKai University Press, China, 2001).
8. Y. Rondelez, M.N. Rager, A. Duprat and O. Reinaud, *J. Am. Chem. Soc*. **124** (2002) 1334.
9. E. Karakhanov, T. Buchneva, A. Maximov and M. Zavertyaeva, *J. Mol. Catal. A–Chem*. **184** (2002) 11.
10. M. Liu, L.S. Li, S.L. Da and Y.Q. Feng, *Talanta* **66** (2005) 479.
11. S.P. Montsenat, Y.L. Zhang and M.W. Isiah, *Anal. Chem*. **69** (1997) 3239.
12. A. Pailleret, N.M. Oliva, S. Ollivier and D.W.M. Arrigan, *J. Electroanal. Chem*. **508** (2001) 81.
13. A. Pailleret and D.W.M. Arrigan, *Langmuir* **18** (2002) 9447.

14. G.W. Diao and W. Zhou, *J. Electroanal. Chem.* **567** (2004) 325.
15. G.W. Diao and Y. Liu, *Electroanalysis* **17** (2005) 1279.
16. C.D. Gutsche, B. Dhawan, K.H. No and R. Muthukrishana, *J. Am. Chem. Soc.* **103** (1981) 3782.
17. C.D. Gutsche, A.l. Iqubal and D. Stewart, *J. Org. Chem.* **51** (1986) 742.
18. C.D. Gutsche, B. Dhawan and M. Leonis, *Org. Synth.* **68** (1990) 234.
19. V. Bocchi, D. Foina, A. Pochini, R. Urgaro and G.D. Andreetti, *Tetrahedron* **38** (1982) 373.
20. C.D. Gutsche and L.G. Lin, *Tetrahedron* **42** (1986) 1633.
21. C.D. Gutsche, J.A. Levine and P.K. Sujeeth, *J. Org. Chem.* **50** (1985) 5801.
22. S. Shinka'i, K. Araki, T. Tsubaki, T. Arimura and O. Manabe, *J. Chem. Soc. Perkin Trans. I* (1987) 2297.
23. S. Shinka'i, S. Mori, T. Tsubaki, T. Sone and O. Manabe, *Tetrahedron Lett.* **25** (1984) 5315.
24. A.J. Bard and L.R. Faulkner, *Electrochemical methods*, 1st ed., (John Wiley & Sons, New York, 1980).
25. D.A. Skoog, D.M. West and F.J. Holler, Fundamentals of Analytical Chemistry, 7th Ed, Saunders College Pub, 1992.